Available online at www.sciencedirect.com
ScienceDirect
Marine Chemistry 106 (2007) 18–32
MARINE CHEMISTRY
www.elsevier.com/locate/marchem

Distribution and biogeochemical behaviour of iron in the East Antarctic sea ice

Delphine Lannuzel [a,*], Véronique Schoemann [b], Jeroen de Jong [a,1], Jean-Louis Tison [c], Lei Chou [a]

[a] *Laboratoire d'Océanographie Chimique et Géochimie des Eaux, Université Libre de Bruxelles, Campus de la Plaine CP 208, Bd. du Triomphe, B-1050 Bruxelles, Belgium*
[b] *Ecologie des Systèmes Aquatiques, Université Libre de Bruxelles, Campus de la Plaine CP 221, Bd. du Triomphe, B-1050 Bruxelles, Belgium*
[c] *Unité de Glaciologie, Université Libre de Bruxelles CP 160/03, 50 Av. F. D. Roosevelt, B-1050 Bruxelles, Belgium*

Received 30 January 2006; received in revised form 16 June 2006; accepted 19 June 2006
Available online 8 August 2006

Abstract

We have attempted to evaluate the relative importance, compared to other possible sources, of sea ice in supplying Fe to East Antarctic surface ocean waters. Samples of snow, brine, seawater and sea ice were collected and processed for Fe analysis during the "ARISE in the East" Antarctic cruise during September–October 2003 (64°–65°S/112°–119°E, *RV Aurora Australis*). Total-dissolvable and dissolved Fe concentrations were measured together with relevant physical, chemical and biological parameters. The most striking feature we observed is that total-dissolvable Fe concentrations in sea ice were up to an order of magnitude higher than those measured in the underlying seawater. Moreover, total-dissolvable Fe in sea ice is more concentrated at cold "winter" type stations than at the warm "spring" ones. This probably results from the enhanced ice permeability as spring arrives, which allows brine drainage within the ice cover and renders exchanges with the water column possible. During the melting period, iron inputs to surface waters from sea ice may represent as much as 70% of the estimated daily total flux into surface seawater when taking into account available data on dust deposition, extraterrestrial iron, vertical diffusion and upwelling. Our results highlight the potentially important contribution of pack ice to the Fe biogeochemical cycle in the East Antarctic oceanic Ecosystem.
© 2006 Elsevier B.V. All rights reserved.

Keywords: Iron biogeochemistry; Fe inputs; Sea ice; East Antarctica

1. Introduction

As an essential nutrient for phytoplankton growth, and hence involved in marine primary productivity and carbon export, iron (Fe) is a key element in the study of ocean–atmosphere biogeochemical interactions. This micro-nutrient has been shown to limit algal growth in "High-Nutrient, Low-Chlorophyll" (HNLC) areas such as the Southern Ocean, where external Fe inputs are low. Potential Fe sources for Antarctic surface waters are: (1) continental and extraterrestrial dust via atmospheric deposition, (2) upwelling and turbulent diffusion, (3) sediment resuspension and lateral advection, and (4) melting sea ice and icebergs (Löscher et al., 1997; Sedwick and DiTullio, 1997; Johnson et al., 1999; Johnson, 2001; Sedwick et al., 2001; Grotti et al., 2005).

* Corresponding author. Tel.: +32 2 650 5278; fax: +32 2 650 5228.
E-mail address: dlannuze@ulb.ac.be (D. Lannuzel).
[1] Current address: Unité de Glaciologie, Université Libre de Bruxelles CP 160/03, 50 Av. F. D. Roosevelt, B-1050 Bruxelles, Belgium.

0304-4203/$ - see front matter © 2006 Elsevier B.V. All rights reserved.
doi:10.1016/j.marchem.2006.06.010

Sea ice covers seasonally large areas of the Southern Ocean and could constitute a significant pool of bioavailable Fe, which in turn could support algal blooms when this ice melts (Sedwick et al., 2000).

The Southern Ocean covers 30% of the global ocean and plays an important role in regulating the Earth's climate as seasonal sea ice formation around Antarctica provide a major drive to the global thermohaline overturning circulation through intermediate and bottom water formation (Sarmiento et al., 1998). Also, low temperatures and strong wind mixing facilitate physical removal of carbon dioxide to the deep sea (Watson and Orr, 2003). In recent years, Fe has been recognized as a key element in ocean biogeochemistry. Martin and Fitzwater (1988) highlighted the role of Fe as a limiting nutrient for phytoplankton growth in HNLC regions of the oceans. Since solubility of Fe in oxygenated seawater is low, and dissolved Fe can be strongly scavenged from the water column due to biological uptake and/or to rapid precipitation and sedimentation of iron oxyhydroxides, dissolved Fe is present in very low concentrations in open ocean surface waters (de Baar and de Jong, 2001). The eolian pathway of Fe may constitute an additional source, but it is typically small in remote ocean regions (Gao et al., 2001; Jickells et al., 2005). Martin (1990) speculated that enhanced dust transport to the Southern Ocean during glacial periods might have fertilized the region, enhancing the "biological carbon pump" and drawing down atmospheric CO_2. Today, atmospheric Fe inputs from the deserts of South Africa, South America, Australia and the Transantarctic Mountains may provide the main inputs of eolian Fe to Antarctic waters. Because of its assumed role as a "dust collector" while covering a large part of the Southern Ocean, sea ice might be a significant pool of bioavailable Fe in Antarctic surface waters, compared to other possible Fe sources.

Sea ice forms as the seawater temperature drops below −1.86 °C, producing frazil ice under agitated conditions or a uniform thin sheet called nilas when the ocean is calm. Congelation or columnar ice may then grow downward by freezing of the water, forming more uniformly oriented crystals (e.g. Weeks and Ackley, 1986; Gow et al., 1998). Snowfalls are frequent in the Southern Ocean, so that a snow layer generally accumulates on top of young sea ice within a few days. Under heavy snow pack, seawater may infiltrate and form the so-called "snow ice". Sea ice textures are important for reconstructing the ice history and for evaluating the conditions under which sea ice was formed. Temporally and spatially, sea ice is a highly heterogeneous medium, with regard to physical, chemical and biological features. Thermodynamics and physical forcing both control ice texture and thickness, thus influencing temperature, salinity, porosity, nutrient content, light penetration and biological activity. These parameters are closely linked, and their relations are highly complex. Thermodynamically, East Antarctic sea ice can grow only to a thickness of 0.5–1 m. However, rafting and ridge building can considerably increase thickness to several meters (e.g. Allison, 1997).

Away from the coast, Antarctic sea ice consists mostly of first-year ice, because most of sea ice melts during the first summer after its formation. The differences in sea ice area in the Southern Ocean between maximum extent in September and minimum extent in February is about 15×10^6 km^2 (Allison, 1997). This vast area provides a habitat for marine organisms, which develop within and beneath the ice column. Although frozen coastal waters (land-fast ice) appear to be a favourable zone for primary production due to land vicinity, open ocean pack ice can sustain high algal biomass as well. Chlorophyll *a* (Chl *a*) levels up to 6 mg/l in land-fast ice (Mc Murdo) and 0.2 mg/l in pack ice (Weddell Sea) have been reported (Arrigo, 2003). Algal communities are observed at different levels within sea ice (e.g. Horner, 1985a). Bottom assemblages are the most common. They grow often under low light conditions and consume major nutrients from the underlying seawater. Internal communities live in brine channels, where salinities and temperatures can be extreme as compared to bottom ice. Surface assemblages are thought to originate from seawater infiltration into the snow pack. Theoretically, sea ice should contain little Fe since it is formed from Fe-deficient waters (Thomas, 2003). But this extreme environment obviously can meet chemical and physical conditions favourable to algal growth. In other words, Fe concentrations must be high enough to sustain biological activity in much of the sea ice.

Sea ice may be a substrate not only for algal production within the ice column itself (surface, internal and bottom assemblages), but also for pelagic phytoplankton communities growing beneath or adjacent to the ice floe. Once the ice starts to melt, Fe may be released and eventually become available for the pelagic algal communities. These phenomena are difficult to quantify, since sea ice Fe data are scarce (Löscher et al., 1997; Grotti et al., 2005; Lannuzel et al., 2006) due in large part to the challenges encountered in this extreme environment with regard to sampling and analysis.

The present study focuses on the biogeochemistry of Fe in Antarctic pack ice in order to assess Fe pools, sources and pathways. The objectives were to characterize the Fe distribution in sea ice, and its associated snow, brine and underlying seawater at 6 stations sampled in the East Antarctic sector of the Southern Ocean during early

austral spring 2003. Iron speciation was determined by measuring the total-dissolvable Fe (TDFe) and dissolved Fe (DFe) pools, and calculating the particulate-dissolvable Fe (PDFe). Based on these data and their possible correlations to sea ice physical properties (ice texture, salinity, temperature), chemistry and biology, we have attempted to assess the possible Fe inputs and pathways, and the importance of sea ice as an Fe source to Southern Ocean surface waters in the seasonal sea ice zone.

2. Material and methods

2.1. Sea ice environment and sample collection

Samples of sea ice and associated snow, brine and underlying seawater were collected during the "ARISE in the East" Antarctic expedition (Antarctic Remote Ice Sensing Experiment, voyage AA03-01, September–October 2003, 64°–65°S/112°–119°E, *RV Aurora Australis*). The 6 stations sampled were located in the seasonal sea ice zone in the deep ocean (Fig. 1A,B).

A full description of the sample collection technique for Fe measurement in sea ice is detailed by Lannuzel et al. (2006). Briefly, snow was first collected in Polyethylene (PE) containers using polypropylene (PP) shovels. A set of closely spaced ice cores (10–20 cm apart from each other) was then sampled on a uniform, levelled sea ice cover, using an electropolished stainless-steel corer previously tested for trace-metal clean conditions in order to assess relevant physical, chemical and biological parameters (temperature, salinity, nutrients and Chl *a*). Cores were stored in a plastic bag (acid-cleaned for the cores dedicated to Fe study) at −28 °C in the dark until further processing. Access holes ("sack holes") were drilled into the sea ice cover at one or two different depths to allow gravity-driven brine collection (ice levels above or below −5 °C threshold when applicable as described by Golden et al., 1998; see Section 3.2). Brines and under ice seawater (0 m, 1 m and 30 m deep) were then pumped up using a portable peristaltic pump (Cole-Parmer, Masterflex E/P) and plastic tubing (sampling system adapted from de Jong et al., 1998). Snow and ice sections of 5–10 cm thickness were melted in trace-metal clean containers in the dark at shipboard ambient temperature.

2.2. Physical and biological parameters

In situ ice temperatures were measured on site using a calibrated probe (TESTO 720) inserted every 5 or 10 cm along the freshly sampled core. Bulk salinity was determined from conductivity using a WP-84-TPS meter. Vertical ice thin-section photographs taken under polarized light (Langway, 1958) indicated ice crystalline shapes and were used as an indicator for ice texture (e.g. columnar vs. granular).

Sea ice sections for Chl *a* determination were melted in seawater filtered through 0.2 μm filters (1:4 volume ratio) to avoid cell lysis by osmotic shock. Chl *a* was quantified fluorimetrically following Yentsch and Menzel (1963) after 90% v:v acetone extraction of the particulate material retained on glass-fibre filters (Whatman GF/F) for 12 h at 4 °C in the dark.

2.3. Iron

Seawater, brine, and melted snow and sea ice samples dedicated for Fe analysis were processed onboard ship. All labware was acid-cleaned according to the procedure described in Lannuzel et al. (2006). Total-dissolvable Fe (TDFe, unfiltered) was stored at pH 1.8 (addition of 100 μl 14 M HNO_3, J.T. Baker, Ultrex for 100 ml of sample) for a period of at least 6 months before Fe measurement by flow injection analysis (FIA), which should dissolve all but the most refractory Fe species. The dissolved Fe fraction (DFe) was collected after filtration through 0.2 μm pore nuclepore polycarbonate (PC) membrane filters, mounted on Sartorius PC filtration devices equipped with Teflon O-rings. The filtrate was acidified to pH 1.8 with 14 M HNO_3 (J.T. Baker, Ultrex) at least 24 h prior to analysis. We adapted a FIA technique (FeLume, Waterville Analytical) to measure TDFe and DFe concentrations in our samples without a pre-concentration step. Analysis of reference material NASS-5 and CASS-3 gives a good agreement with the certified values and detection limit (3σ of the blank) is on average 0.12 nM (Lannuzel et al., 2006). Particulate-dissolvable Fe (PDFe) refers to the difference in concentration between TDFe and DFe.

3. Results

3.1. Ice texture

Sea ice thickness at our selected sampling sites ranged from 0.3 m (station XIII) to 0.8 m (station V) thickness. Thin section observations reveal a typical pack ice structure, with snow ice and/or frazil ice, underlain by congelation ice (Fig. 2). Station IV apparently underwent a similar genesis as station IX, with about 15 cm of frazil ice growing then into columnar ice (~30 cm). Both stations V and VII show a thick snow ice layer (~20 cm deep) with contrasted snow metamorphism, then a frazil ice layer followed by a columnar structure. Stations XII and XIII display a somewhat more complex sequence of

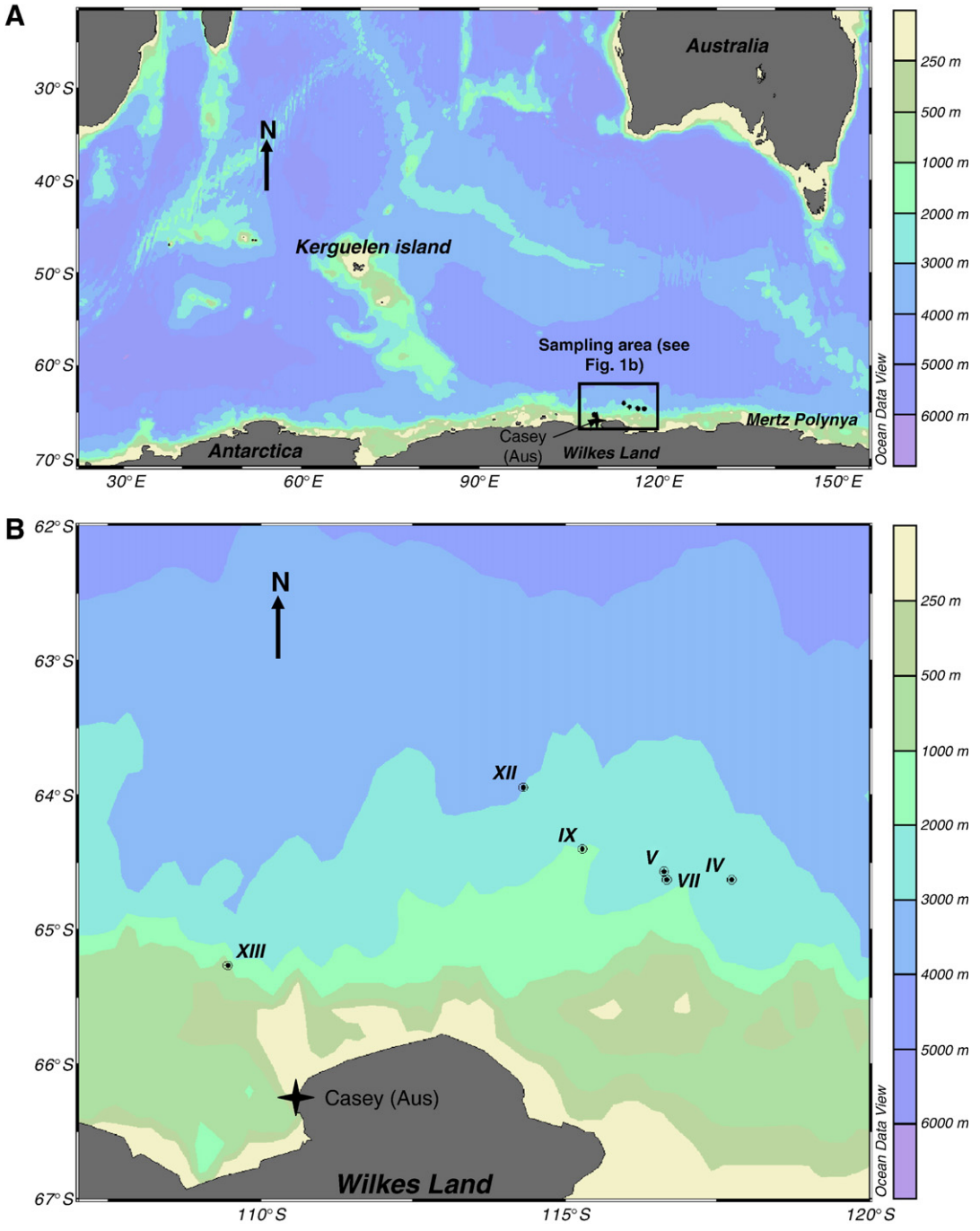

Fig. 1. (A and B) Location of the sampling area (Schlitzer, R., Ocean Data View, http://www.awi-bremerhaven.de/GEO/ODV, 2005).

genetic processes, probably involving rafting. This is suggested by the repeated occurrence of bent columnar crystals at station XII and the "flattened" frazil ice crystals in the lower part of the core XIII (Fig. 2). Stations IV, V, VII and IX are located at the same latitude (64.3°S), whereas stations XII and XIII are located at 63.6°S and 65.2°S, respectively.

3.2. Temperature, bulk ice salinity, brine volume and Chl a profiles

In sea ice, the upper layer is colder than the bottom layer because of the relatively low air temperature compared to underlying seawater. Sea ice indeed exhibits a marked transition in its fluid transport

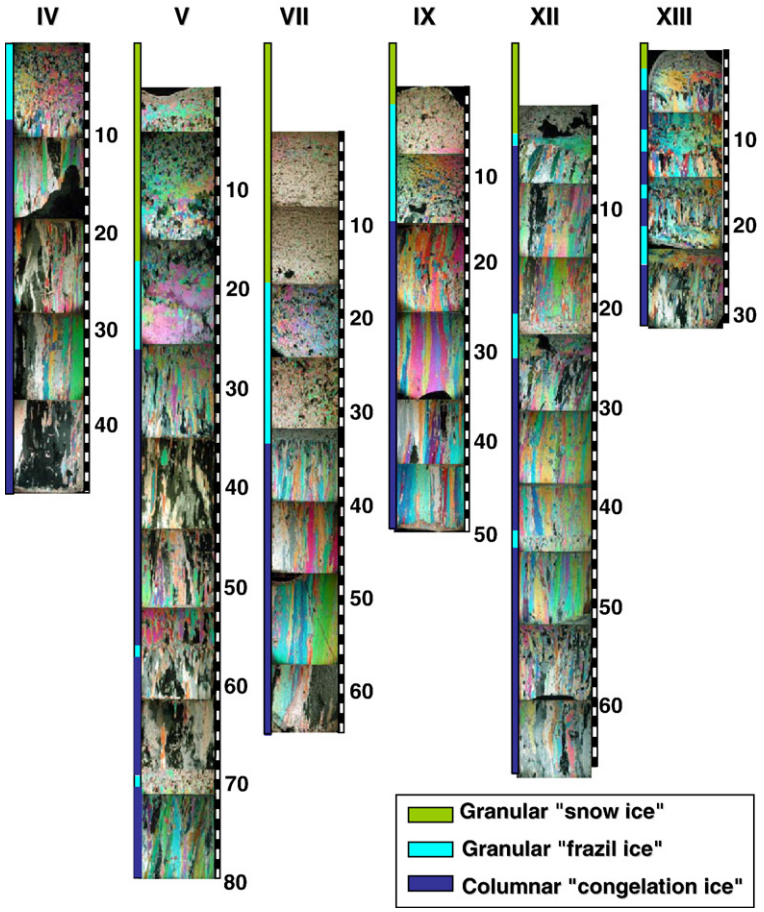

Fig. 2. Ice textures from vertical thin sections, viewed under crossed polarizers of ice cores for each stations. Depths have been adjusted so that snow thickness is taken into account.

properties at a brine volume fraction of about 5%, which roughly corresponds to a −5 °C ice temperature at a bulk ice salinity of 5 (Golden et al., 1998). For brine volume fractions higher than 5%, brine inclusions become interconnected and can carry heat and nutrients through the ice, whereas for lower porosities the ice is impermeable. Golden et al. (1998) referred this threshold behaviour as the "law of fives".

Temperature profiles allow a possible classification in terms of the thermal stages at our stations (Fig. 3). Station IV had the coldest ice, with its upper half exhibiting the lowest ice temperatures. Then ice at

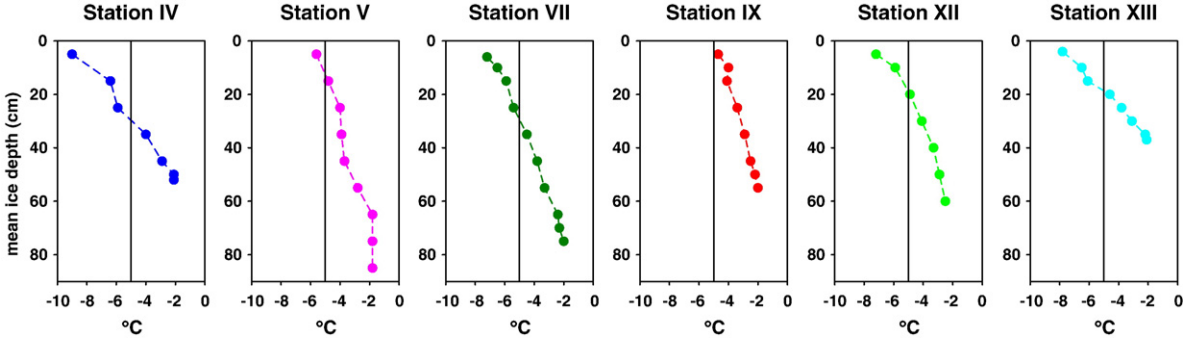

Fig. 3. Temperature (°C) profiles in sea ice. The −5 °C critical temperature is indicated by the vertical line.

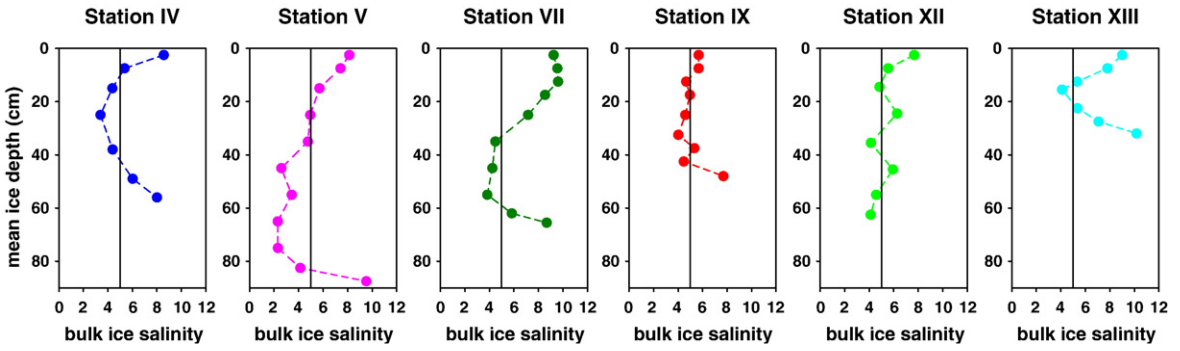

Fig. 4. Bulk salinity profiles in sea ice. The critical salinity 5 is indicated by the vertical line.

stations VII, XII and XIII appeared to be in a later seasonal stage compared to station IV, as ice temperatures were slightly higher in the upper half of the ice cover. Finally, both stations V and IX showed a warmer regime as most of the ice cover was above −5 °C.

Most stations showed the typical C-shaped bulk salinity profile described in many other field studies of sea ice (e.g. Nakawo and Sinha, 1981; Weeks and Ackley, 1986; Eicken, 1992, 1998) (Fig. 4). Higher salinities at the top result from enhanced initial entrapment under faster growth rates, brine expulsion upwards on cooling, and eventually seawater infiltration in snow ice, later in the season. Lower salinities in the middle levels reflect enhanced salt rejection after initial entrapment under slower growth rates and brine drainage, whilst higher salinities in the warmer bottom layers result from higher porosities and lack of brine drainage in the fragile skeletal layer. Sea salts tend to be more easily trapped in surface frazil ice because of its rapid formation (a few hours to a few days, depending on air temperature), whereas congelation ice forms slowly (weeks to months) and expels salts more efficiently. This contrast supports the previous assumption of ice rafting at station XII, which shows the repetition of such a sequence with depth.

The evolutionary stages described from the various temperatures profiles are also shown in the calculated brine volume fraction (V_b/V=brine volume/bulk ice volume; Eicken, 2003) profiles (Fig. 5). This variable is of critical importance since brine drainage within the ice towards the underlying water can be regarded as a key physical process for Fe transfer. Station IV clearly shows $V_b/V<5\%$ in the upper ice column because cold ice temperature favours smaller brine volumes and higher brine salinity. On the contrary, the lower section of this core indicates increased porosity and permeability (V_b/V being $>5\%$), and possible exchanges with underlying seawater. In contrast, ice porosity at stations V, VII and IX was considerably higher, with brine volumes typically being $\geq 5\%$ along all cores. Stations XII and XIII displayed a somewhat intermediate profile in the upper half of the ice cover. One should bear in mind that air temperature, ice thickness and texture, snow cover and solar irradiance all contribute to the control of ice temperature, salinity and permeability. Within a few hours, meteorological conditions may act together and affect the brine volumes at different locations along the core. It is thus not surprising that the complex links between different physical properties render a clear seasonal characterization for all stations difficult, especially in the spring.

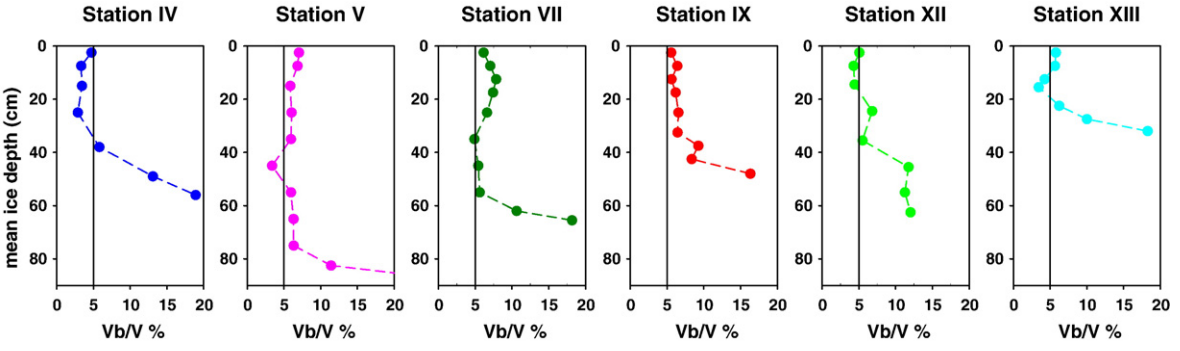

Fig. 5. Brine volume fraction V_b/V (%) profiles in sea ice. The 5% critical brine volume is indicated by the vertical line.

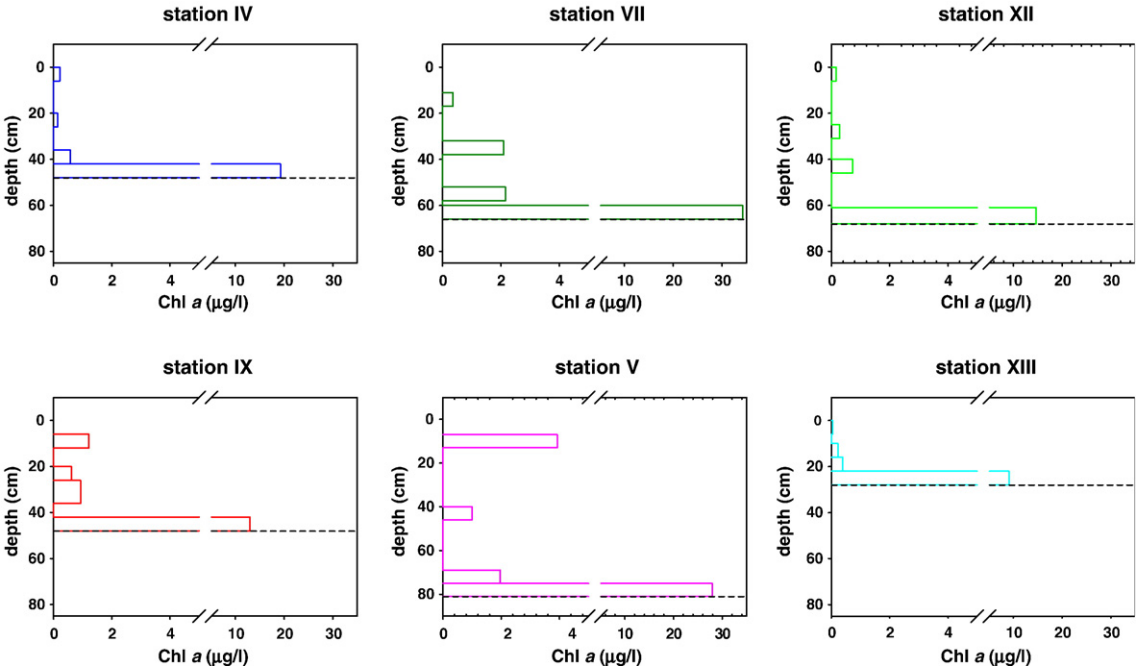

Fig. 6. Chlorophyll *a* (µg/l) profiles in four sea ice sections. The dashed horizontal black line represents the ice–water interface.

Chl *a* profiles indicate maximum values (i.e. from 9.1 to 34.2 µg/l) were systematically located in the lower portions of the ice at all stations (Fig. 6). Algal biomass was however also observed at other levels in the cores of stations V, VII and IX. This probably reflects increased ice permeability at these stations, supplying major

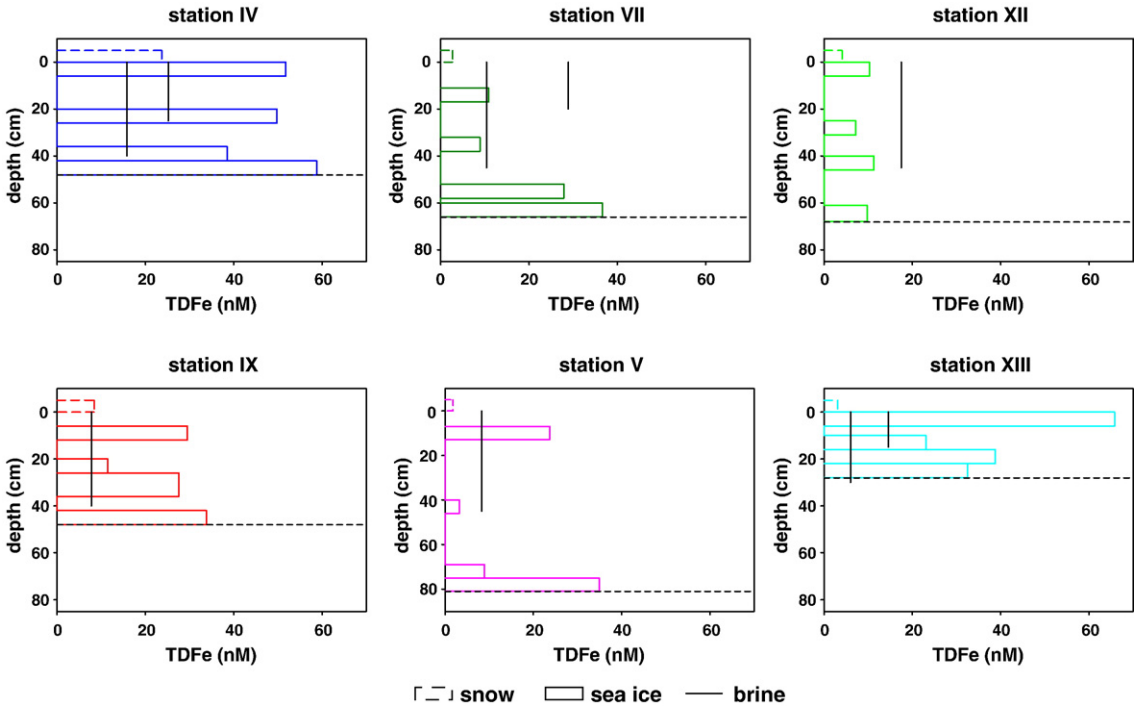

Fig. 7. TDFe (nM) profiles in four sea ice sections (solid bars), snow (dotted bars) and brines (vertical lines for cold<−5 °C shallow brine and warm>−5 °C deep brine).

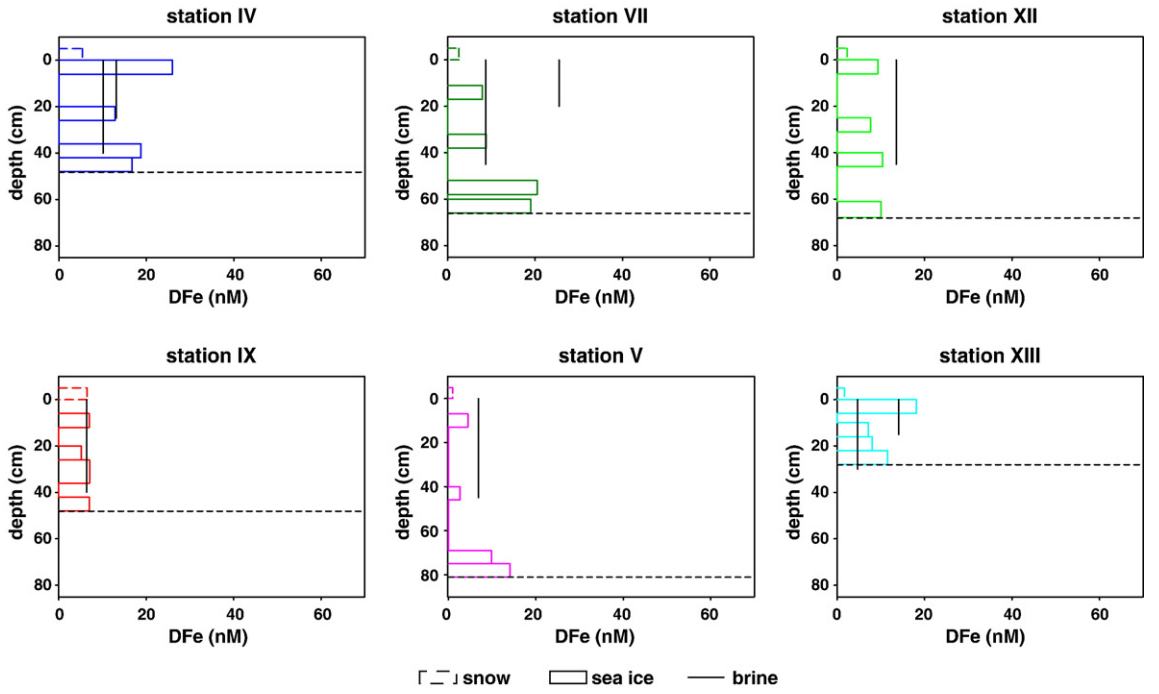

Fig. 8. DFe (nM) profiles in four sea ice sections (solid bars), snow (dotted bars) and brines (vertical lines for cold < −5 °C shallow brine and warm > −5 °C deep brine).

nutrients from seawater and possibly Fe from the sea ice, in addition to improved light conditions.

In light of the physical parameters and Chl *a* profiles, stations V and IX can be regarded as typical "spring" stations as revealed by ice temperatures > −5 °C and brine volume fractions > 5% throughout the ice cover. The latter physical characteristic allows vertical ice–water exchanges, thus algal development along the whole core (Fig. 6). Note that in the case of station V, one cannot preclude snow ice formation (i.e. seawater infiltration into the snow pack) as an efficient process for initial algal "seeding" and major nutrients enrichment of the top ice layer. In contrast, station IV is more likely a "winter" type station: Figs. 3 and 5 demonstrate that the ice is impermeable to brine exchange in the upper part of the ice cover, therefore preventing algal development in the upper ice (Fig. 6). Stations VII, XII and XIII exhibit a transitional regime, with the upper 30 cm of stations XII and XIII still reflecting low permeability.

3.3. Spatial and temporal distribution of Fe

Figs. 7–9 show the profiles of TDFe, DFe and PDFe in our East Antarctic pack ice cores (bars), including surface snow (dashed bars). "Sack hole" brine (> −5 °C and < −5 °C when present) concentrations are indicated by solid vertical lines.

Our results tend to show relatively high Fe contents in the sea ice compared to under-ice seawater (Table 1). Generally, sea ice and brines exhibit the highest Fe levels, followed by snow. These three media are more concentrated in Fe than the underlying seawater. The ranges are: 3.3–65.8 nM TDFe and 2.6–26.0 nM DFe in sea ice, 6.0–28.9 nM TDFe and 4.7–25.5 nM DFe in brines, 1.8–23.7 nM TDFe and 1.0–6.5 nM DFe in snow, and 1.2–3.8 nM TDFe and 1.1–4.5 nM DFe in under-ice seawater. Seawater shows a major DFe fraction compared to the sea ice as reflected by DFe percentages of 78±23% (1σ, n=15) in seawater and 60±32% (1σ, n=24) in sea ice.

On the whole, station IV exhibits higher levels of TDFe, DFe and PDFe in sea ice, brines and snow compared to other sampled stations (Figs. 7–9). Based on the data collected at 4 levels along the core, we vertically integrated the concentrations of TDFe, DFe and PDFe per core at each station. This provides an estimate of a mean bulk concentration of Fe in ice at each station (Table 2). The mean TDFe bulk concentration estimated for station IV is the highest at 48.9 nM, followed by stations XIII and IX, where average integrated TDFe concentrations are 40.7 and 24.0 nM, respectively. The averaged integrated bulk concentrations of Fe (1σ standard deviation) estimated in sea ice for all stations investigated are respectively 25.7±15.8 nM TDFe, 10.7±4.6 nM DFe and 15.0±12.8 nM PDFe.

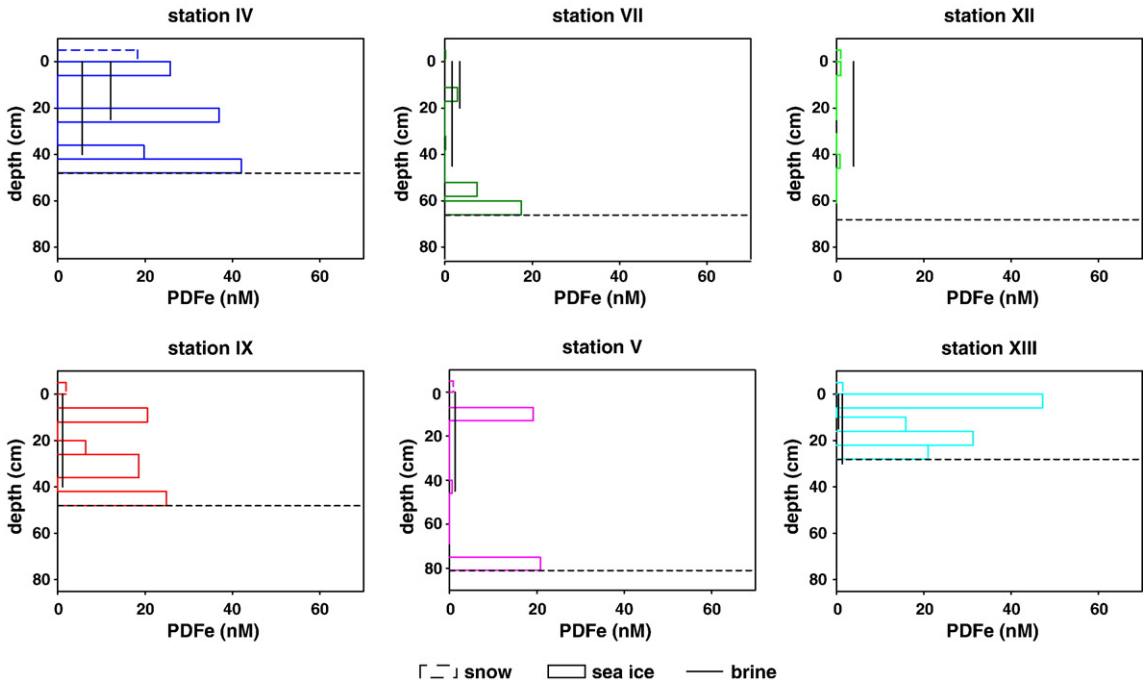

Fig. 9. PDFe (nM) profiles in four sea ice sections (solid bars), snow (dotted bars) and brines (vertical lines for cold < −5 °C shallow brine and warm > −5 °C deep brine).

In the same ice core, the Fe concentration measured in cold shallow brine is typically higher than in warm deep brine; for example, TDFe at station VII is 28.9 nM at 20 cm and 10.4 nM at 45 cm sampled depths (Table 1). Another notable feature is that most of the Fe of the brines is in the dissolved phase, as can be observed at station XIII, where DFe and TDFe are 14.1 nM and 14.6 nM at 15 cm depth. As a result, DFe represents on average 78±14% (1σ, n=9) of TDFe in brines. Both brines and seawater therefore exhibit a high DFe percentage of TDFe, as compared to sea ice.

Finally, Fe levels in snow are relatively low, with a somewhat higher value at "winter" station IV (Table 1); concentrations of TDFe range from 1.8 nM (station XIII) to 23.7 nM (station IV). Dissolved Fe is on the average 56±26% (1σ, n=6) of TDFe in the snow.

4. Discussion

4.1. Distribution and biogeochemical behaviour of Fe

4.1.1. Sea ice, seawater and snow

Patchiness can be a recurrent factor within the same ice floe (Eicken et al., 1991). Sea ice is indeed a highly dynamic and heterogeneous medium in terms of thickness, texture, nutrients distribution, gas content, light penetration, biological activity and probably Fe distribution. As we present here a spatial study of cores collected on different ice floes, it is important to compare stations exhibiting similar ice structure. Hypothetically, stations IV, V, VII and IX, which are located at the same latitude and similar water depth, should have received similar Fe inputs from atmospheric deposition and advection from the continent shelf. Ice at station XII (farther from the coast) and station XIII (closer to the coast) probably reflect rafting processes; it is therefore difficult to assess whether stations XII and XIII received the same external Fe inputs as stations IV, V, VII and IX. Based on similarities in ice textures, we thus compare here below station IV to station IX, station V to station VII, and finally stations XII to XIII.

Station IV clearly shows high DFe and TDFe contents in the sea ice compared to station IX. This is probably due to the difference in the stage of seasonal ice evolution. Station IV can be associated with "winter" type ice in terms of ice temperature, brine volume and Chl *a* profiles (Figs. 3, 5, and 6). In contrast, station IX ice demonstrates "spring" type features, which could favour brine drainage and Fe transfer from the ice pack to the water column below. Besides thermodynamic controls, biological activity is likely to have a strong impact on Fe distribution in the sea ice environment. In nutrient-replete Antarctic waters, light conditions are improving in spring and Fe may become available from the sea ice as it starts to

Table 1
TDFe (nM), DFe (nM), PDFe (nM), temperature (°C) and salinity at the visited stations

		Depth	Ice texture	*T* (°C)	Salinity	TDFe	DFe	PDFe
Station IV	Snow					23.7	5.4	18.3
01-oct-03	Sea ice	0–6 cm	Frazil	−8.9	8.6	51.8	26.0	25.8
64°37.7′S		20–26 cm	Columnar	−5.9	3.6	49.8	12.9	37.0
117°44.5′E		36–42 cm	Columnar	−3.7	4.4	38.5	18.8	19.7
		42–48 cm	Bottom	−3.0	6.0	58.8	16.7	42.1
	Brine	0–25 cm		−8.2	103.5	25.2	13.1	12.1
		0–40 cm		−6.0	89.9	15.8	10.1	5.6
	Seawater	0 m			34.3	3.0	2.4	0.5
		1 m			34.3	2.7	2.4	0.3
		30 m			34.3	1.4	1.1	0.2
Station V	Snow					1.8	1.0	0.9
07-oct-03	Sea ice	7–13 cm	Snow ice	−5.2	6.6	23.7	4.5	19.2
64°34.0′S		40–46 cm	Columnar	−3.5	3.1	3.3	2.6	0.6
116°37.8′E		69–75 cm	Columnar	−1.9	2.3	8.9	9.8	[a]
		75–81 cm	Bottom	−1.8	3.3	34.9	14.1	20.8
	Brine	0–45 cm			78.6	8.2	6.9	1.3
	Seawater	0 m			34.3	3.0	1.3	1.7
		1 m			34.2	2.3	1.3	1.0
Station VII	Snow					2.7	2.6	0.1
09-oct-03	Sea ice	11–17 cm	Snow ice	−6.2	9.1	10.9	8.0	2.9
64°38.0′S		32–38 cm	Columnar	−4.7	4.5	8.9	8.8	0.1
116°40.7′E		52–58 cm	Columnar	−3.2	3.8	27.9	20.5	7.4
		60–66 cm	Bottom	−2.7	7.3	36.6	19.0	17.6
	Brine	0–20 cm			89.1	28.9	25.5	3.4
		0–45 cm		−6.7	80.1	10.4	8.7	1.7
	Seawater	0 m			34.2	2.0	1.1	0.9
		1 m			34.2	2.9	1.9	1.0
Station IX	Snow					8.4	6.5	1.9
11-oct-03	Sea ice	6–12 cm	Frazil	−4.3	5.2	29.5	8.0	21.5
64°24.1′S		20–26 cm	Columnar	−3.6	4.7	11.5	4.8	6.7
115°17.5′E		36–42 cm	Columnar	−2.8	4.9	27.6	7.1	20.5
		42–48 cm	Bottom	−2.4	6.1	33.8	7.0	26.8
	Brine	0–40 cm		−2.8	61.5	7.6	6.4	1.1
	Seawater	0 m			34.3	1.9	1.7	0.2
		1 m			34.3	3.3	1.9	1.4
		30 m				2.1	1.7	0.4
Station XII	Snow					4.1	2.3	1.8
14-oct-03	Sea ice	0–6 cm	Snow ice	−6.7	7.7	10.3	9.3	1.0
63°56.2′S		25–31 cm	Columnar	−4.7	5.2	7.2	7.6	[a]
114°19.4′E		40–46 cm	Frazil/columnar	−3.4	5.9	11.3	10.4	0.9
		61–68 cm	Bottom	−1.9	4.1	9.8	10.0	[a]
	Brine	0–40 cm		−3.8	63.0	17.4	13.5	3.9
	Seawater	0 m			34.2	2.2	2.1	0.1
		1 m			34.2	3.8	4.5	[a]
Station XIII	Snow					3.1	1.7	1.4
20-oct-03	Sea ice	0–6 cm	Frazil/columnar	−7.9	9.0	65.8	18.1	47.6
65°16.1′S		10–16 cm	Frazil/columnar	−6.1	5.3	23.1	7.2	15.9
109°27.8′E		16–22 cm	Frazil/columnar	−5.1	4.7	38.8	8.0	30.8
		22–28 cm	Bottom	−4.0	6.2	32.5	11.5	21.0
	Brine	0–15 cm		−6.0	93.7	14.6	14.1	0.5
		0–25 cm		−4.2	88.0	6.0	4.7	1.4
	Seawater	0 m			34.3	2.1	1.5	0.6
		1 m			34.3	1.7	1.4	0.3
		30 m			34.3	1.2	1.3	[a]

The sampling date and location are indicated for each site, in addition to media, sampling depths and sea ice textures.
[a] Not detectable within measurement error.

Table 2
Estimated averaged bulk concentrations (nM) of total-dissolvable Fe (TDFe), dissolved Fe (DFe) and particulate-dissolvable Fe (PDFe)

Stations	TDFe (nM)	DFe (nM)	PDFe (nM)
Station IV	48.9	18.3	30.6
Station V	13.5	5.6	7.9
Station VII	17.7	13.1	4.6
Station IX	24.0	6.7	17.3
Station XII	9.5	9.3	0.3
Station XIII	40.7	11.4	29.2

melt. All environmental conditions are then met to favour an algal bloom. Although internal melting has probably occurred, lower DFe and relatively high PDFe concentrations in sea ice at station IX together with increases in Chl *a* levels suggest biological Fe uptake within the ice (see Table 1 and Fig. 7). Decreases in major nutrients concentrations throughout the ice core between the winter and spring type stations are also observed (ranges for station IV and IX are respectively: 0.4–14.4 μM and 0.4–5.65 μM NO_3, 1.3–12.8 and 2.2–10.2 μM $Si(OH)_4$, and 0.04–10.4 and 0.03–4.0 μM PO_4; data not shown). This comparison is only valid if the two stations had similar initial inventory; a situation that is likely since similar ice structures suggest similar sea ice history, and thus similar Fe accumulation processes.

In the same way, station VII can be regarded as a colder station with regard to station V (see temperature profile in Fig. 3). Chl *a* profiles (Fig. 6) and apparent DFe "drawdown" (Table 2) support the idea that station V is in a later stage of the seasonal ice evolution compared to station VII.

Stations XII and XIII both underwent a perturbed genesis as revealed by the succession of frazil and congelation ice sections which lead to strong differences in thickness and probably age. Comparisons of Fe distributions between these two stations are therefore difficult, as we cannot assume that initial Fe stocks were similar. Note, however, that station XII shows a larger proportion of ice with increased permeability, suggesting that it is in a later seasonal stage as compared to station XIII.

To summarize, comparisons of station IV with station IX, station VII with station V, and station XIII with station XII suggest that, as the spring progresses, both ice melting and biological activity are important processes in controlling the distribution and speciation of Fe in the sea ice.

The inferred release of Fe from the ice pack as spring progresses is not obvious from the seawater Fe profiles. This may reflect rapid scavenging, vertical mixing and/or diffusion below the ice, both leading to Fe removal from the upper water column and transfer to deeper water. Seawater Fe concentrations are nevertheless relatively high compared to levels usually encountered in ice-free surface waters (e.g. 0.05–0.3 nM DFe, de Jong et al., 1998; 0.1 nM DFe, Bowie et al., 2001).

Reported Fe concentration levels in snow from previous studies suggest that this medium could potentially contribute to the high Fe values observed in sea ice and underlying seawater (Westerlund and Öhman, 1991; Löscher et al., 1997; Edwards et al., 1998). However, the snow sampled at our locations did not, in general, exhibit Fe concentrations as high as those we observed in sea ice, possibly reflecting the remoteness of our study area with respect to dust sources, compared to other investigated sites. Our snow TDFe values are consistent with other published data for the East Antarctic sector, ranging from 1.2 to 31.7 nM (Edwards and Sedwick, 2001). Long-term deposition of aerosol Fe could be responsible for the high Fe values in the sea ice topmost layers, with the low ice temperature in the upper half of the sea ice cover preventing transfer of this surface enrichment to the lower levels via the brine system (e.g. station IV).

Table 3
Upper ocean iron input estimates during sea ice melting

		Remarks
Sea ice formation Fe uptake		
Winter TDFe (nM)	49	Station IV
Winter DFe (nM)	18	Station IV
Thickness (m)	0.5	Station IV
Residence time of sea ice (9 months) in days	274	
Required TDFe flux to sea ice (μmol/m^2/day)	0.09	External supply 0.13, Table 4
Required DFe flux to sea ice (μmol/m^2/day)	0.03	External supply 0.28, Table 4
Sea ice melting Fe release		
TDFe inventory (μmol/m^2)	24.5	0.49 nM TDFe addition to upper 50 m if melted at once
DFe inventory (μmol/m^2)	9	
Melting time (day)	30	
Release TDFe (μmol/m^2/day)	0.82	
Release DFe (μmol/m^2/day)	0.30	
DFe total flux to the upper ocean during sea ice melting	μmol/m^2/day	
Atmospheric/ extraterrestrial	0.0016	
Vertical diffusion	0.01	
Upwelling	0.12	
Sea ice melting	0.30	
Total	0.43	

Table 4
Estimates of iron input to the upper Antarctic Ocean

$J_{diff} = Kz \times d[DFe]/dz$
$J_{upwelling} = v_{upwelling} \times [DFe]_{deep}$
$J_{tot} = J_{atm} + J_{space} + J_{diff} + J_{upwelling}$

		Remarks	References
Aerosol flux J_{atm}			
Dust input (mg/m^2/year)	5	Range 1–10	Duce and Tindale, 1991
TDFe flux (μmol/m^2/day)	0.011	Assuming 4.3% Fe content	Wedepohl, 1995
DFe flux (μmol/m^2/day)	0.0005	Solubility mineral dust 5%	Baker et al., 2006
TDFe flux (μmol/m^2/day)	0.003	SSIZ, 32% mean solubility	Edwards and Sedwick, 2001
DFe flux (μmol/m^2/day)	0.0010		Edwards and Sedwick, 2001
Average DFe flux (μmol/m^2/day)	0.0008		
Extraterrestrial flux J_{space}			
DFe (μmol/m^2/day)	0.0008	Assumed 100% soluble	Johnson, 2001
Vertical diffusion J_{diff}			
K_z (m^2/s)	3.0e−05	ACC (56°S, 15°W)	de Baar et al., 1995
d[DFe]/dz (μmol/m^4)	0.006		
DFe flux (μmol/m^2/day)	0.016		
TDFe flux (μmol/m^2/day)	0.031[a, b]		
K_z (m^2/s)	2.4e−05	SOIREE (61°S, 140°E)	Law et al., 2003
d[DFe]/dz (μmol/m^4)	0.003		Bowie et al., 2001
DFe flux (μmol/m^2/day)	0.006		
TDFe flux (μmol/m^2/day)	0.012[a, b]		
K_z (m^2/s)	6.6e−05	FeCycle (46°S, 179°E)	Boyd et al., 2005
d[DFe]/dz (μmol/m^4)	0.00066		
DFe flux (μmol/m^2/day)	0.004		
TDFe flux (μmol/m^2/day)	0.008[a, b]		
Average DFe flux (μmol/m^2/day)	0.009		
Average TDFe flux (μmol/m^2/day)	0.017		
Upwelling $J_{upwelling}$			
Upwelling velocity (m/s)	1.5e−06	ACC (56°S, 15°W)	de Baar et al., 1995
Deep water concentration (nM)	1		
DFe flux (μmol/m^2/day)	0.13		
TDFe flux (μmol/m^2/day)	0.26[a]		
Surface (m^2)	1.08e+13[c]		Watson, 2001
Upwelling flux (Sv)	25		
Deep water concentration (nM)	0.6		
DFe flux (μmol/m^2/day)	0.12		
TDFe flux (μmol/m^2/day)	0.24[a]		
Average DFe flux(μmol/m^2/day)	0.12		
Average TDFe flux (μmol/m^2/day)	0.25		
Total flux J_{tot}			
Average DFe flux (μmol/m^2/day)	0.13		
Average TDFe flux (μmol/m^2/day)	0.28		

[a] Assuming TDFe = 2 × DFe.
[b] Assuming the same vertical diffusivity for TDFe and DFe.
[c] Surface based on biogeochemical provinces from Longhurst et al. (1995).

4.1.2. Brines

Concentrations of TDFe and DFe in sea ice were up to two orders of magnitude higher than in typical Antarctic seawater. When seawater freezes, sea-salts are expelled together with other impurities (e.g. gases, particles) into the brine system and the water below (Eicken, 1998). In this context, and given the mean calculated brine volumes at our stations (V_b/V=3–27%, Fig. 5) the TDFe and DFe concentrations should be about 4 to 33 times higher in brine than in bulk sea ice. However, we observed similar levels in both media. A potential explanation for this apparent discrepancy is that the brine collection technique ("sack-hole") might lead to an underestimation of the particulate Fe content in brines. Due to its high particle affinity, the Fe associated with micro-organisms and derived organic matter could remain attached to the walls of the brine channels during sample collection, thus not be recovered (Krembs et al., 2001). For the same reason, it might well be that Fe does not behave in the same way as other nutrients during sea ice formation. Iron would not be expelled into the liquid brine, but could use the solid phase, such as wall channels, pure ice crystals or even particulate matter (organic or inorganic), as sorptive surfaces. Comparing TDFe and DFe concentrations in sea ice and brine at station XIII provides evidence to support this hypothesis. Indeed, TDFe and DFe concentrations are nearly identical in the brine, while TDFe is considerably higher than DFe in the ice. This suggests that particulate Fe might not be easily drained into the brine sack hole, and is perhaps retained in the ice medium.

The difference in Fe content between shallow (<−5 °C) and deep (>−5 °C) brines could be a consequence of brine exchanges between the bottom ice cover and the surface seawater. Density difference between brine and underlying seawater can initiate brine convection, as rising temperatures in the bottom ice re-establish connection between brine in the lower sea ice and the seawater below. Comparison of winter and spring brine profiles also tends to show a decline in salinity and Fe, as spring progresses. This can be explained by both brine dilution by freshwater from melting pure ice and/or dilution by seawater due to brine convection.

4.2. Fe and ice texture relationships

Ice texture provides information on the ice growth history, and may help in deciphering Fe sources and pathways in the ice column. Iron accumulates within pack ice at concentrations clearly exceeding that of the underlying seawater. In the case of planktonic organisms, enrichment has been attributed to physical concentration mechanisms, via scavenging by frazil ice crystals rising through the water column (Garrison et al., 1983, 1989; Reimnitz et al., 1990). In this process, suspended organisms are thought to adhere to individual ice crystals (frazil ice) that develop and rise in the surface waters. Alternatively, micro-organism particulates may be concentrated by wave fields pumping water through the freshly formed frazil ice layer, causing particles to become attached to, or trapped between, the ice crystals (Weissenberger and Grossmann, 1998). Thus, sea ice genesis could eventually lead to physical enrichment of particulate or colloidal Fe within the pack ice, together with planktonic organisms. However, such enrichment would mainly be confined to frazil ice layers as it is probably the case for stations IV and XIII.

Within our cores, however, no clear overall relationship was observed between ice texture and Fe content (Table 1). For example at station IV, TDFe is 51.8 nM in frazil ice, 49.8 nM and 38.5 nM in columnar sections, and 58.8 nM in bottom ice (also of columnar nature). Bottom ice TDFe enrichment could be caused by phytoplankton DFe uptake in the bottom ice assemblages. On one hand, we might expect higher Fe levels in snow ice, because of accumulation of atmospheric deposition, and in frazil ice via planktonic enrichment. But on the other hand, columnar ice should more efficiently expel sea salts and particles during formation, especially at depth, and therefore might not accumulate Fe. Our observations support neither scenario, and point toward the need for further research on the processes of Fe enrichment and transfer in sea ice.

4.3. Requirements and potential sources for Fe inputs to the sea ice cover

In our investigation, station IV can be regarded as a "winter" type station and its iron content might thus be taken as representative of the initial Fe distribution before significant melting (Table 2). Considering a 9-month residence time of 0.5 m thick ice, the required Fe flux into sea ice in order to accumulate 49 nM TDFe and 18 nM DFe would be 0.09 μmol TDFe/m^2/day and 0.03 μmol DFe/m^2/day (Table 3).

Based on data from the literature, we attempted to estimate Fe inputs to the Southern Ocean surface waters from various possible sources including atmospheric dust deposition (J_{atm}), extraterrestrial input (J_{space}), vertical diffusion (J_{diff}) and upwelling ($J_{upwelling}$). The calculations suggest a possible total flux of 0.28 μmol TDFe/m^2/day and 0.13 μmol DFe/m^2/day to the surface Antarctic waters (Table 4). Amongst the considered sources, upwelling should dominate the Fe inputs, accounting for about 90% of the total. This means that potential sources

of Fe to the upper waters of the Southern Ocean are sufficient to account for the total DFe and TDFe trapped in pack ice based on our data (Table 4).

4.4. Importance of sea ice as a source of Fe to Antarctic surface waters

Table 3 shows estimated TDFe and DFe fluxes from melting East Antarctic pack ice to the upper water column. For an ice floe of 0.5 m thickness containing an average of 49 nM TDFe and 18 nM DFe (station IV), and assuming a melting period of 1 month, the estimated releases to the upper ocean would be 0.82 μmol TDFe/m^2/day and 0.30 μmol DFe/m^2/day – this equates to a 0.49 nM TDFe addition over a 50 m mixed layer. During spring melting, compared to other sources, sea ice could thus represent a significant Fe source to the Antarctic surface waters (Table 4). When integrating atmospheric dust and extra-terrestrial deposition (0.0016 μmol DFe/m^2/day), vertical diffusion (0.01 μmol DFe/m^2/day), upwelling (0.12 μmol DFe/m^2/day) and sea ice melting (0.30 μmol DFe/m^2/day), the total DFe flux to the ocean surface would be 0.43 μmol DFe/m^2/day (Table 3), of which sea ice could represent 70% of the total input. Hence, sea ice melting during austral spring may be important, as a source of Fe, in favouring ice edge spring blooms.

5. Conclusions

The East Antarctic pack ice investigated in the present study reveals high Fe contents in sea ice as compared to under-ice seawater. Both thermodynamic and biological processes are likely key factors controlling the Fe distribution, as spring progresses and the ice warms. Comparison of Fe content and ice texture sheds some light on possible Fe pathways to pack ice. Complementary field data and laboratory experiments simulating ice growth could provide further mechanistic insights into the enrichment processes for Fe in the sea ice environment. Melting sea ice may provide a significant input of Fe to Antarctic surface waters during spring, in comparison to other sources, and may thus play an important role in fuelling algal blooms in the seasonal ice zone.

Acknowledgments

The authors would like to thank the Australian Antarctic Division, especially Ian Allison (Expedition Leader) and Rob Massom (Chief Scientist), for inviting us on the "ARISE in the East" endeavour. We are also grateful to the captain and crew of the *RV Aurora Australis* for their logistic assistance throughout the duration of the cruise. The support from Bruno Delille for field assistance, Anne Trevena for ice core sub-sampling and salinity measurements and Marie-Line Sauvée for processing samples for nutrient analysis is greatly acknowledged. The two anonymous reviewers are greatly acknowledged for their valuable comments, which improved the clarity of our paper. This work was funded by the Belgian French Community (ARC contract no. 2/07-287) and by the Belgian Federal Science Policy Office (contracts EV/12/7E and SD/CA/03A). This is also a contribution to the SOLAS international research initiative, the European Network of Excellence EUR-OCEANS (contract no. 511106-2) and to the European Integrated Project CarboOcean (contract no. 511176-2).

References

Arrigo, K.R., 2003. Primary production in sea ice. The importance of sea ice: an overview. In: Thomas, D.N., Dieckmann, G.S. (Eds.), Sea Ice – An Introduction to its Physics, Chemistry, Biology and Geology. Blackwell Science, Oxford, pp. 143–183.

Allison, I., 1997. Physical processes determining the Antarctic sea ice environment. Aust. J. Phys. 50 (4), 759–771.

Baker, A.R., Jickells, T.D., Witt, M., Linge, K.L., 2006. Trends in the solubility of iron, aluminium, manganese and phosphorus in aerosol collected over the Atlantic Ocean. Mar. Chem. 98 (1), 43–58.

Bowie, A.R., Maldonado, M.T., Frew, R.D., Croot, P.L., Achterberg, E.P., Mantoura, R.F.C., Worsfold, P.J., Law, C.S., Boyd, P.W., 2001. The fate of added iron during a mesoscale fertilisation experiment in the Southern Ocean. Deep-Sea Res., Part 2, Top. Stud. Oceanogr. 48, 2703–2743.

Boyd, P.W., Law, C.S., Hutchins, C.S., Abraham, D.A., Croot, E.R., Ellwood, P.L., Frew, M., Hadfield, R.D., Hall, M., Handy, J., Hare, S., Higgins, C., Hill, J., Hunter, P., LeBlanc, K.A., Maldonado, K., McKay, M.T., Mioni, R.M., Oliver, C., Pickmere, M., Pinkerton, S., Safi, M., Sander, K., Sanudo-Wilhelmy, S., Smith, S.A., Strzepek, M., Tovar-Sanchez, R., Wilhelm, S.W., 2005. FeCycle: Attempting an iron biogeochemical budget from a mesoscale SF_6 tracer experiment in unperturbed low iron waters. Glob. Biogeochem. Cycles 19, GB4S20, doi:10.1029/2005GB002494.

de Baar, H.J.W., de Jong, J.T.M., 2001. Distribution, sources and sinks of iron in seawater. In: Turner, D.R., Hunter, K.H. (Eds.), The Biogeochemistry of Iron in Seawater, IUPAC Series on Analytical and Physical Chemistry of Environmental Systems, vol. 7, pp. 123–253.

de Baar, H.J.W., de Jong, J.T.M., Bakker, D.C.E., Loscher, B.M., Veth, C., Bathmann, U., Smetacek, V., 1995. Importance of iron for phytoplankton spring blooms and CO_2 drawdown in the Southern Ocean. Nature 373, 412–415.

de Jong, J.T.M., den Das, J., Bathmann, U., Stoll, M.H.C., Kattner, G., Nolting, R.F., de Baar, H.J.W., 1998. Dissolved iron at subnanomolar levels in the Southern Ocean as determined by ship-board analysis. Anal. Chim. Acta 377, 113–124.

Duce, R.A., Tindale, N.W., 1991. Atmospheric transport of iron and its deposition in the ocean. Limnol. Oceanogr. 36, 1715–1726.

Edwards, R., Sedwick, P.N., 2001. Iron in East Antarctic snow: implications for atmospheric iron deposition and algal production in Antarctic waters. Geophys. Res. Lett. 28 (20), 3907–3910.

Edwards, R., Sedwick, P.N., Morgan, V., Boutron, C.F., Hong, S., 1998. Iron in ice cores from Law Dome, East Antarctica: implications for past deposition of aerosol iron. Ann. Glaciol. 27, 365–370.

Eicken, H., 1992. Salinity profiles of Antarctic sea ice: field data and model results. J. Geophys. Res. 97 (C10), 15545–15557.

Eicken, H., 1998. Factors determining microstructures, salinity and stable-isotope composition of Antarctic sea ice: deriving modes and rates of ice growth in the Weddell Sea. In: Jeffries, M.O. (Ed.), Antarctic Sea Ice: Physical Processes, Interactions and Variability. Antarct. Res. Ser., vol. 74. AGU, Washington, D.C., pp. 89–122.

Eicken, H., 2003. From the microscopic, to the macroscopic, to the regional scale: growth, microstructure, and properties of sea ice. In: Thomas, D.N., Dieckmann, G.S. (Eds.), Sea Ice – An introduction to its physics, chemistry, biology and geology. Blackwell Science, Oxford, pp. 22–83.

Eicken, H., Lange, M.A., Dieckmann, G.S., 1991. Spatial variability of sea ice properties in the northwestern Weddell Sea. J. Geophys. Res. 96 (C6), 10603–10615.

Gao, Y., Kaufman, Y.J., Tanre, D., Kolber, D., Falkowski, P.G., 2001. Seasonal distributions of aeolian iron fluxes to the global ocean. Geophys. Res. Lett. 28, 29–32.

Garrison, D.L., Ackley, S.F., Buck, K.R., 1983. A physical mechanism for establishing algal populations in frazil ice. Nature 306, 363–365.

Garrison, D.L., Close, A.R., Reimnitz, E., 1989. Algae concentrated by frazil ice: evidence from laboratory experiments and field measurement. Antarct. Sci. 1 (4), 313–316.

Golden, K.M., Ackley, S.F., Lytle, V.I., 1998. The percolation phase transition in sea ice. Science 282, 2238–2241.

Gow, A.J., Ackley, S.F., Govoni, J.W., Weeks, W.F., 1998. Physical and structural properties of land-fastice in Mc Murdo Sound, Antarctica. In: Jeffries, M.O. (Ed.), Antarctic Sea Ice: Physical Processes, Interactions and Variability. Antarct. Res. Ser., vol. 74. AGU, Washington, D.C., pp. 355–374.

Grotti, M., Soggia, F., Ianni, C., Frache, R., 2005. Trace metals distributions in coastal sea ice of Terra Nova Bay, Ross Sea, Antarctica. Antarct. Sci. 17 (2), 289–300.

Horner, R.A., 1985a. History of ice algal investigations. In: Horner, R.A. (Ed.), Sea Ice Biota. CRC Press, Boca Raton, pp. 1–19.

Jickells, T.D., An, Z.S., Anderson, K.K., Baker, A.R., Bergametti, G., Brooks, N., Cao, J.J., Boyd, P.W., Duce, R.A., Hunter, K.A., Kawahata, H., Kubilay, N., La Roche, J., Liss, P.S., Mahowald, N., Prospero, J.M., Ridgwell, A.J., Tegen, I., Torres, R., 2005. Global iron connections between desert dust, ocean biogeochemistry and climate. Science 308, 67–71.

Krembs, C., Mock, T., Gradinger, R., 2001. A mesocosm study of physical–biological interactions in artificial sea ice: effects of brine channel surface evolution and brine movement on algal biomass. Polar Biol. 24, 356–364.

Johnson, K.S., 2001. Iron supply and demand to the upper ocean: is extraterrestrial dust a significant source of bioavailable iron? Glob. Biogeochem. Cycles 15 (1), 61–63.

Johnson, K.S., Chavez, F.P., Frederich, G.E., 1999. Continental-shelf sediment as a primary source of iron for coastal phytoplankton. Nature 398, 697–700.

Langway, C.C., 1958. Ice fabrics and the universal stage. CRREL Technical, vol. 62. USA Cold Regions Research and Engineering Laboratory.

Lannuzel, D., de Jong, J.T.M., Schoemann, V., Trevena, A., Tison, J.-L., Chou, L., 2006. Development of a sampling and flow injection analysis technique for iron determination in the sea ice environment. Anal. Chim. Acta 556 (2), 476–483.

Law, C.S., Abraham, E.R., Watson, A.J., Liddicoat, M.I., 2003. Vertical eddy diffusion and nutrient supply to the surface mixed layer of the Antarctic Circumpolar Current. J. Geophys. Res. 108 (C8), 3272.

Longhurst, A., Sathyendranath, S., Platt, T., Caverhill, C., 1995. An estimate of global primary production in the ocean from satellite radiometer data. J. Plankton Res. 17 (6), 1245–1271.

Löscher, B.M., de Baar, H.J.W., de Jong, J.T.M., Veth, C., Dehairs, F., 1997. The distribution of Fe in the Antarctic Circumpolar Current. Deep-Sea Res., Part 2, Top. Stud. Oceanogr. 44, 143–187.

Martin, J.H., Fitzwater, S.E., 1988. Iron deficiency limits phytoplankton growth in the north-east Pacific subarctic. Nature 331, 341–343.

Martin, J.H., 1990. Glacial–interglacial CO_2 change: the iron hypothesis. Paleoceanography 5, 1–13.

Nakawo, M., Sinha, N.K., 1981. Growth rate and salinity profile of first-year sea ice in the Arctic. J. Glaciol. 27 (96), 315–330.

Reimnitz, E., Kempema, E.W., Wefer, W.S., Clayton, J.R., Payne, J.R., 1990. Suspended-matter scavenging by rising frazil ice. In: Ackley, S.F., Weeks, W.F. (Eds.), Sea Ice Properties and Processes: Proceedings of the Sea Ice Symposium. CRREL Monograph, vol. 90-1. Cold Region Research and Engineering Laboratory, Hanover, pp. 97–100.

Sarmiento, J.L., Hughes, T.M.C., Stouffer, R.J., Manabe, S., 1998. Simulated response of the ocean carbon cycling to anthropogenic carbon warming. Nature 393, 245.

Sedwick, P.N., DiTullio, G.R., 1997. Regulation of algal blooms in Antarctic shelf waters by the release of iron from melting sea ice. Geophys. Res. Lett. 24 (20), 2515–2518.

Sedwick, P.N., DiTullio, G.R., Mackey, D.J., 2000. Iron and manganese in the Ross Sea, Antarctica: seasonal iron limitation in Antarctic shelf waters. J. Geophys. Res. 105, 11321–11336.

Sedwick, P.N., Harris, P.T., Robertson, L.G., McMurtry, G.M., Cremer, M.D., Robinson, P., 2001. Holocene sediment records from the continental shelf of Mac, Robertson Land, East Antarctica. Paleoceanography 16 (2), 212–225.

Thomas, D., 2003. Iron limitation in the Southern Ocean. Science 302, 565.

Watson, A.J., 2001. Iron limitation in the oceans. In: Turner, D.R., Hunter, K.H. (Eds.), The Biogeochemistry of Iron in Seawater. IUPAC Series on Analytical and Physical Chemistry of Environmental Systems, vol. 7, pp. 9–39.

Watson, A.J., Orr, J.C., 2003. Carbon dioxide fluxes in the global ocean. In: Fasham, M.J.R. (Ed.), Ocean Biogeochemistry: The Role of the Ocean Carbon Cycle in Global Change. Springer-Verlag, Berlin.

Wedepohl, K.H., 1995. The composition of the continental crust. Geochim. Cosmochim. Acta 59, 1217–1232.

Weeks, W.F., Ackley, S.F., 1986. The growth, structure and properties of sea ice. In: Untersteiner, N. (Ed.), The Geophysics of Sea Ice. NATO ASI Series, pp. 9–164.

Weissenberger, J., Grossmann, S., 1998. Experimental formation of sea ice: importance of water circulation and wave action for incorporation of phytoplankton and bacteria. Polar Biol. 20, 178–188.

Westerlund, S., Öhman, P., 1991. Iron in the water column of the Weddell Sea. Mar. Chem. 35, 199–217.

Yentsch, C.S., Menzel, D.W., 1963. A method for the determination of phytoplankton chlorophyll and phaeophytine by fluorescence. Deep-Sea Res. 10, 221–231.